



## LATERAL PERFORMANCE OF PRECAST POST-TENSIONED CONCRETE FILLED FIBER TUBES

M.A. ElGawady<sup>1</sup> H. Dawood<sup>2</sup>

### ABSTRACT

Recently a new construction system consisted of segmental precast post-tensioned concrete filled fiber tubes (PPT-CFFT) was developed at Washington State University. Both single-column and two-column bridge-bents were subjected to cyclic loads. The tests showed that the PPT-CFFT can safely and effectively resist lateral cyclic forces. This paper discusses finite element modeling and analysis of the developed system. Three dimensional nonlinear finite element analyses using Abaqus\Standard have been performed. A stress-strain relationship for confined concrete was used to model the concrete. The post-tensioning tendons were modeled with beam elements. The model was calibrated against cyclic tests on single-column pier. The model was able to capture the general performance of the column. However, careful consideration must be taken when selecting the type of the contact surface between the core concrete and FRP as well as between the core concrete and the foundation. The results indicated that increasing the applied post-tensioning force increases ultimate strength and decreases ultimate displacement. Additionally, for the same post-tensioning force, increasing the rebar cross sectional area increased the post-elastic stiffness and ultimate strength without affecting the ultimate displacement.

### Introduction

Correctly designed and detailed reinforced concrete structures, under the prevailing capacity design concepts, are anticipated to exhibit inelastic response leading to structural damage and permanent drift at the conclusion of ground motion excitation. This requires long-term closure of highways while expensive repairs, or even complete replacements, are carried out. Following the Kobe earthquake (Japan 1994), over 100 reinforced concrete bridge columns were demolished due to a residual drift ratio in excess of 1.75% [Lee and Billington 2010].

Recent research has shown that residual displacement and damage to reinforced concrete structures linked to seismic loads can be minimized by implementing a precast post-tensioning (PPT) construction system. The potentials of this system were highlighted in the U.S. PRESSS research program where a self-centering system when implemented with precast elements demonstrated superior seismic performance [Priestley et al. 1999].

---

<sup>1</sup> Assistant Professor, Dept. of Civil and Environmental Engineering, Washington State University, Pullman, WA, [melgawady@wsu.edu](mailto:melgawady@wsu.edu)

<sup>2</sup> Graduate Research Assistant, Dept. of Civil and Environmental Engineering, Washington State University, Pullman, WA

## Literature Review

Segmental precast column construction is an economic option to accelerate bridge construction in regions of low seismicity in the USA. Examples of bridges constructed with segmental columns include the Louetta Road Overpass (SH-249, Texas), Linn Cove Viaduct (Grandfather Mountain, North Carolina), Sunshine Skyway Bridge (I-275, Florida), Varina-Enon Bridge (I-295, Virginia), John T. Collinson Rail Bridge (Pensacola, Florida), Seven Mile Bridge (Tallahassee, Florida), and the Chesapeake and Delaware Canal Bridge (St. Georges, Delaware). However, the applications of this construction system in active seismic regions in the USA are limited due to concerns about its seismic response [Kwan and Billington 2003].

A segmental PPT bridge pier will rock back and forth during ground motion excitation and re-center upon unloading as a result of the restoring nature of the applied post-tensioning force. This concept has been implemented in the South Rangitikei rail bridge in New Zealand, completed in 1981. In this case, the bridge piers were designed to lift off of the foundation under seismic loading. Recently, tests showed that PPT segmental columns can safely resist lateral cyclic forces [Chou and Chen 2006, Ou et al. 2006, Hewes and Priestley 2002]. PPT columns were capable of withstanding large nonlinear displacements without experiencing significant or sudden loss of strength. The nonlinear behavior resulted from opening of the interface joints between segments as well as material nonlinearity. Hence, residual displacements and damage at the conclusion of these tests were small compared to typical monolithic reinforced concrete columns. Increasing the post-tensioning force significantly reduced the residual displacement but increase concrete damage.

Tests on post-tensioned precast bridge piers showed limited hysteretic energy dissipation [Chou and Chen 2006, Hewes and Priestley 2002]. To overcome this drawback, the post-tensioned precast piers were supplied by internal mild steel at the interfaces between the segments as well as between the bottom segment and foundation. However, the provided mild steel increased the residual displacements and damage compared to columns without mild steel. External energy dissipaters “fuses” were also used for bridge piers [Marriott et al. 2009, Rouse 2009, Chou and Chen 2006]. These external simple yield-dissipaters significantly increased the energy dissipation. Another approach to improve the seismic performance of PPT bridge piers is to use a neoprene pads between the pier and its foundation. ElGawady et al. (2005 and 2006) showed that there is an interaction between the rocking response and the foundation interface material. Using soft rubber above a reinforced concrete base significantly reduced the velocity demand on the column. The energy dissipation increased as well since the soft rubber changed the energy dissipation function from a discrete to a continuous function.

Recently, concrete filled fiber reinforced polymer tubes (CFFT) has been successfully used as pier columns, girders, and piles in different field applications by several State Departments of Transportations [Fam et al. 2003]. Zhu et al. [2006] investigated the seismic behavior of one PPT concrete column encased in concrete filled fiber reinforced polymer tubes (PPT-CFFT). The column reached a drift of 13% without losing its strength and the test was stopped because the actuator reached its displacement capacity.

ElGawady et al. [2010(a) and 2010(b)] and ElGawady and Booker [2009] investigated the cyclic behavior of hybrid segmental bridge bents consisting of precast post-tensioned concrete filled fiber reinforced polymer tubes (PPT-CFFT). Both single-column and two-column bents were tested. The columns were constructed by stacking precast concrete filled fiber

reinforced polymer tube (CFFT) segments one on top of the other and then connecting the assembly structurally with unbonded post-tensioned Dywidag bar passing through a PVC duct located in the center of the segments. The fiber reinforced polymer tube was used as shear and confinement reinforcement for the concrete as well as a stay-in-place formwork.

### Finite Element Modeling

This paper presents a three dimensional finite element model for single-column PPT-CFFT. Fig. 1 shows an example of a segmented single-column PPT-CFFT specimen during testing at Washington State University (ElGawady et al. 2009).

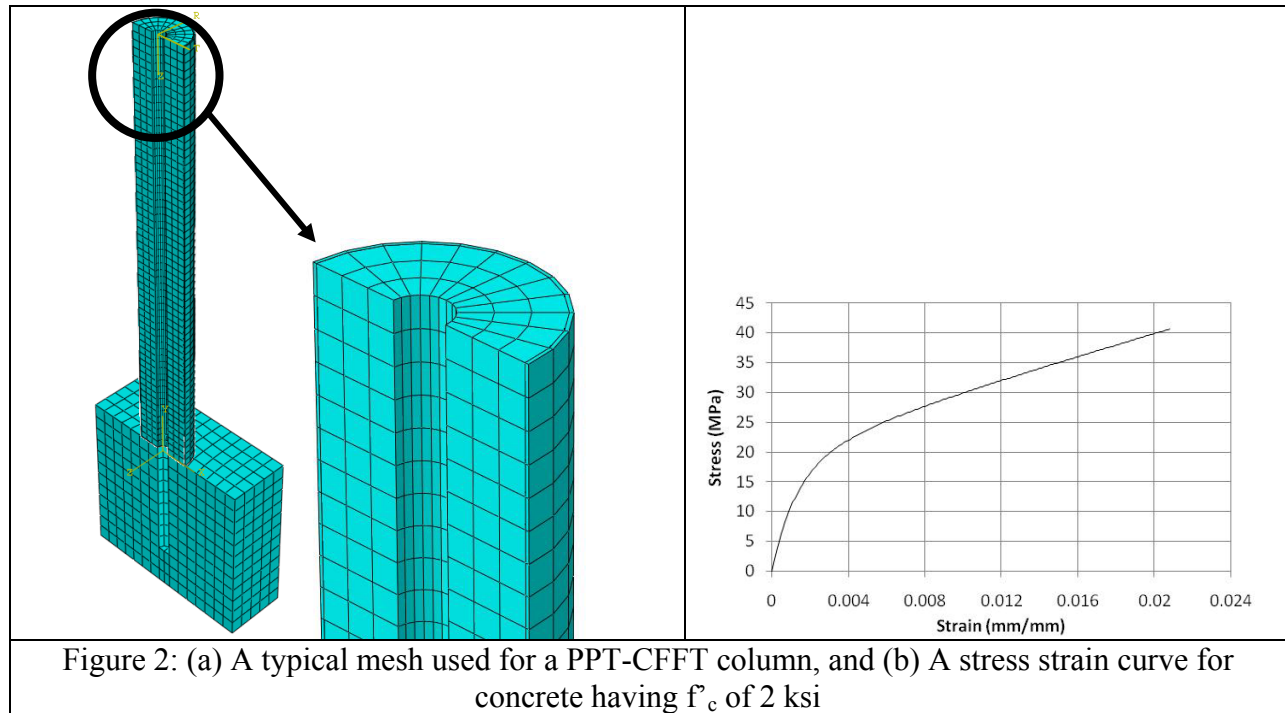


Figure 1: Segmented single-column specimen during testing

### Constitutive Theories and Mesh

This section briefly outlines the constitutive theories used in the finite element analyses. A thorough discussion pertaining to the definition of the theories utilized is presented by Dawood (2010).

Standard eight-node, fully integrated, 3D linear stress/displacement continuum brick elements (C3D8) were used for modeling the core concrete, foundation, and FRP tube. During the analysis, the columns were meshed such that each element height was approximately 25.4 mm. The element length in the column radial direction was also 25.4 mm (Fig.2). Standard linear space shear flexible beam elements (B31) were used to model the post-tensioning bar with an approximate element length of 50 mm.



### Concrete

The concrete damaged plasticity model was used to define behavior of the concrete. Compression behavior of the concrete was defined by concrete compressive stress and corresponding inelastic strain data. For a given concrete strength and FRP characteristics, the confined stress-strain relationship of the core concrete was first evaluated using a simple model developed by Samaan et al. (1998). An example of the stress-total strain relationship is provided in Fig. 2(b), where the unconfined concrete compressive strength was 13.8 MPa. This relationship was prescribed by tabular data which specifies the stress and corresponding values of plastic strain.

Poisson's ratio was specified as 0.2. Five parameters are required to define the yield surface, flow potential, and viscosity parameters for the concrete damaged plasticity constitutive model: the dilation angle in degrees, the flow potential eccentricity, the ratio of initial equibiaxial compressive yield stress to initial uniaxial compressive yield stress, the ratio of the second stress invariant on the tensile meridian to that on the compressive meridian, and the viscosity parameter that defines visco-plastic regularization. The aforementioned parameters were set to  $15^\circ$ , 0, 0, 0, and 0, respectively.

Concrete tension stiffening was prescribed using tabular form as a function of the cracking strain. The maximum permissible tension stress in the concrete was calculated using ACI 318-08 as shown in Equation 1.

$$f_t = 7.5 \sqrt{f'_c} \quad (\text{Eq. 1})$$

### Post-tension bar

The classic Mises metal plasticity model was used to define the behavior of the post-tensioning bar. Material properties for the bar including elastic modulus, yield strength, Poisson ratio,

ultimate strain, ultimate stress were provided by the bar manufacturer. The post-tensioned bar was attached to the tip of the column and the foundation using an embedded element constraint.

### **Behavior at Contact**

The tangential contact between any two parts of the model e.g. post-tensioning bar/PVC tube, FRP/concrete or concrete/concrete, was modeled using standard hard contact with finite sliding formulation and node to surface discretization. Coefficient of frictions of 0, 0.5, and 0.1 were selected for post-tensioning bar/PVC tube, concrete/concrete and concrete/FRP tube surfaces, respectively. The normal components of contact of the FRP tube/foundation and core concrete/foundation were split into two stages. Prior to interface joint opening, a linear penalty hard contact with a stiffness scale factor of 2.0 was used to minimize penetration. Once opening of the interface joint occurs, the cracks begin to form in the grout due to stress concentration, thus the stiffness scale factor was decreased to 0.01, allowing for some penetration.

### **Loading**

Three loading steps were used for the analysis of the column. The first analysis step applied the post-tensioning force at the tip of the column using a stress-type initial condition on the rebar. During the second step, the gravity load was applied as a traction force on the column tip in the negative y-direction (Fig. 2a). The final loading step consisted of a monotonic push in the positive x-direction provided in the form of a uniformly distributed ramped traction pressure applied to the side surfaces of the column tip. It should be noted that the gravity load was a non-following surface traction while the monotonic push load was specified to follow the rotation of the structure.

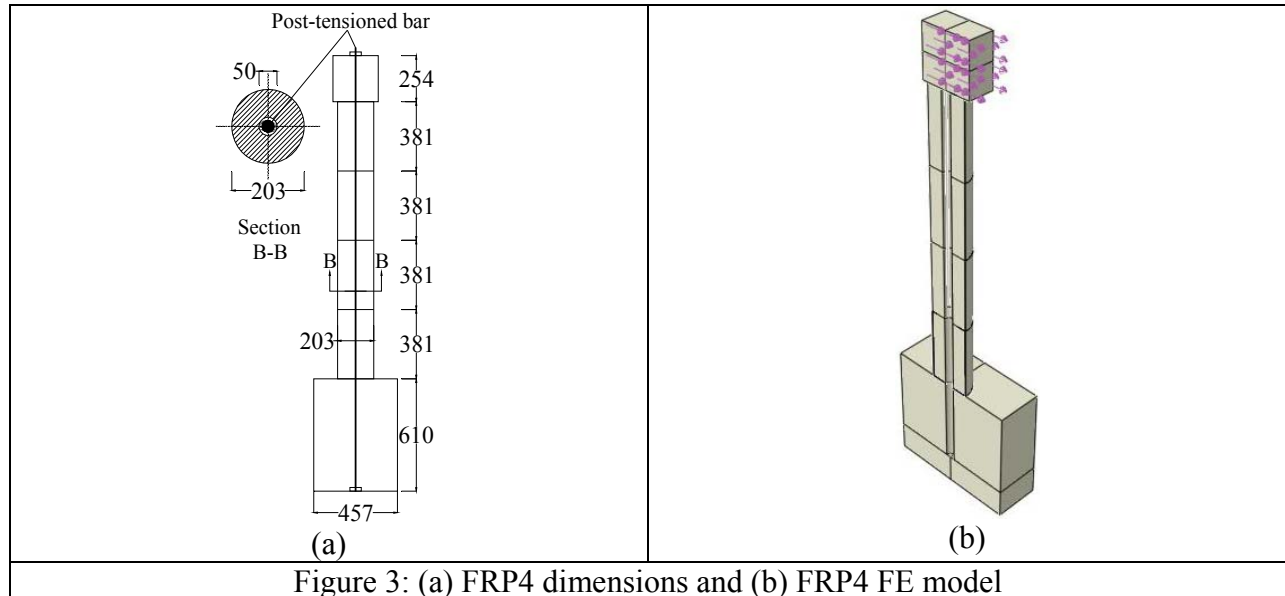
### **Boundary and Initial Conditions**

To simulate a cantilevered structure, the  $U_x$ ,  $U_y$ , and  $U_z$  degrees of freedom (DOF) (Fig. 2a) were constrained for all the nodes at the bottom surface of the foundation while the  $U_x$  and  $U_y$  DOF at the top of the column were unrestrained to simulate a free end. A symmetry (ZSYMM) boundary condition was also applied to the employed plane of symmetry.

### **Model Calibration**

Tests on single-column piers performed at Washington State University (WSU) [ElGawady et al. 2009], were used to calibrate the finite element model presented in this paper. Specimen FRP4 was selected for calibration of the finite element model. This specimen consisted of 4 segments of CFFT. The total height of the column was 1650 mm and was tested as a cantilevered column. An overview of the test specimens are provided in Fig. 1 and Fig. 3. The measured concrete compressive strength and elastic modulus were 13.8 MPa, and 13617 MPa, respectively. The wall thickness of the FRP tube was 3.18 mm and the tensile strength and elastic modulus of the FRP were taken as 63 MPa and 13.8 GPa, respectively. The concrete strength and elastic modulus for the foundation and segments were assumed to be the same. During testing, a loading stub was used to apply the lateral load. The stub material was modeled using a linear elastic concrete definition. The lateral forces were applied to the sides of the loading stub (Fig. 3b), as previously described. The post-tensioning bar had a diameter of 31.75 mm with an elastic

modulus of 172 GPa. The applied post-tensioning force after elastic shortening was approximately 2500 kN. During the experimental work, the post-tensioning bar passed through a 50 mm PVC duct located in the center of the column. A similar duct was provided in the FE model. The post-tensioning bar was embedded in the loading stub and foundation using an embedded element constraint. A grout layer having a thickness of 6.25 mm was provided between the first segment and the concrete foundation during the experimental work.



## Results

Fig. 4 shows the deformed shape of the column measured during the experimental work as well as the response obtained from the finite element analysis. A comparison of the FEA results and experimental results for the lateral load-displacement relationship at the middle of the loading stub is presented in Fig. 5. As shown in these figures, the FEA model was able to capture the general performance of the tested specimen. The performance of both test specimens was significantly governed by the nonlinear geometry due to opening of the interface joints. Once the interface joint opened there was a softening in the post-elastic stiffness. Once the depth of the interface joint opening exceeded half of the column diameter an increase in the post-tensioning force occurred, resulting in a positive post-elastic stiffness.

Fig. 5 illustrates that the FEA model predictions of the initial and post-yield stiffness agree well with the experimental results, however, the FEA model was less ductile than the experimental test. The analytical model predicted that the concrete at the column toe would reach its ultimate strength at a lateral displacement of approximately 80 mm (black dot in Fig. 5). However, if the limit on the concrete ultimate stress was ignored, the FEA model was able to achieve convergence and withstand a larger displacement. In this case, the penetration of the column reached 6.25 mm, the thickness of the grout layer, at a lateral displacement of approximately 300 mm, and the analysis was stopped. During the experimental work, the grout layer was severely damaged during testing. In addition, minor cracks appeared in the concrete core inside the FRP tube at the interface between the first segment and the foundation. The experimental test was stopped when the hydraulic actuator reached its stroke capacity.



Figure 4: Deformed shape of FRP4 (a) from the experimental work, and (b) from the FE modeling

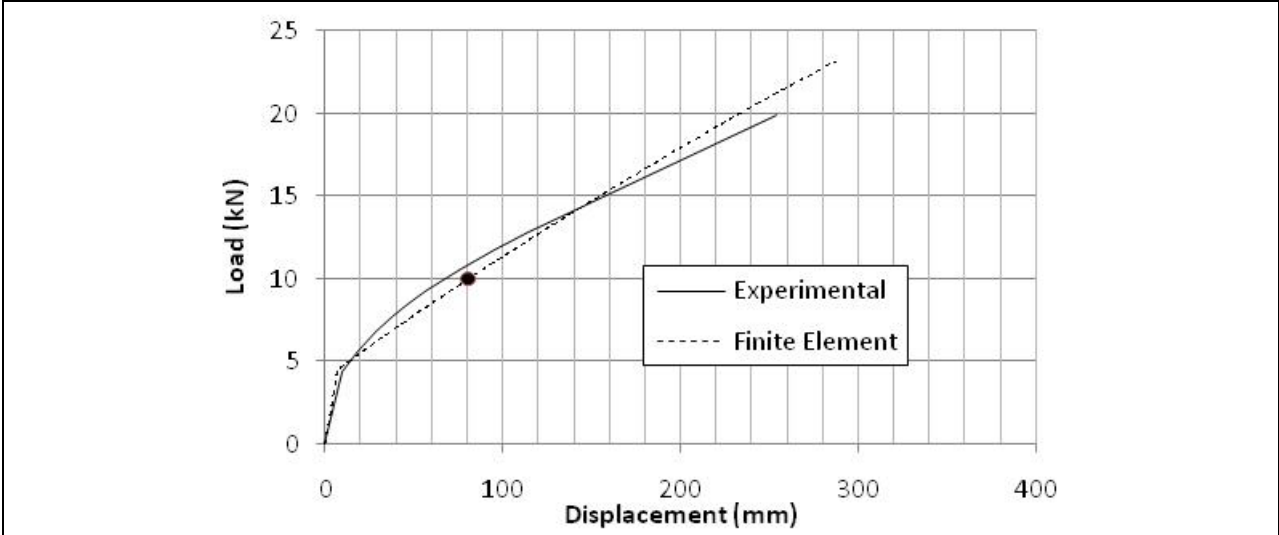


Figure 5: Lateral force vs. lateral displacement from the finite element model and the experimental results

**Parametric Study**

Three parameters were varied through a series of analyses to understand their effect on the performance of PPT-CFFT columns. The applied external axial load, post-tensioning force and initial post-tensioning stress in the rebar were the parameters investigated. Table 1 summarizes the different values used for the parametric study.

For the parametric study, a cantilever column having the same dimensions as the one described above was investigated. However, a concrete having a compressive strength of 41.4 MPa was used. In addition, a nominal external axial load of 86.5 kN, representing the service axial load on the column, was applied. The nominal post-tensioning force was 137.7 kN, which corresponds to an applied axial stress of 660 MPa.

As shown in Fig. 6, increasing the applied axial load or post-tensioning force increased the first crack load as well as the ultimate load. However, the ultimate displacement was found to decrease when the applied axial load or the post-tensioning force is increased. The figure also shows that the applied axial load or post-tensioning force has a negligible effect on the post-elastic stiffness. This occurred since the rebars did not experience any plastic deformation..

**TABLE 1 Summary of The Parametric Study Variables**

Parameter	Description	Value Used
External Vertical Load	Nominal : induce stress on concrete = 7% of $f'_c$	86.5 kN
	Increased : induce stress on concrete = 10% of $f'_c$	123.5 kN
	Decreased: induce stress on concrete = 5% of $f'_c$	61.8 kN
Initial Post-tensioning Load	Nominal: induce stress on concrete = 11% of $f'_c$	137.7 kN
	Increased: induce stress on concrete = 15% of $f'_c$	187.7 kN
	Increased: induce stress on concrete = 20% of $f'_c$	250.4 kN
Initial Post-tensioning Stress in the Rebar	Nominal: induce stress on concrete = 20% of $f_y$	175.5 N/mm <sup>2*</sup>
	Increased: induce stress on concrete = 40% of $f_y$	350.5 N/mm <sup>2*</sup>
	Decreased: induce stress on concrete = 10% of $f_y$	87.5 N/mm <sup>2*</sup>

\*Corresponding to post-tensioning load of 137.7 kN

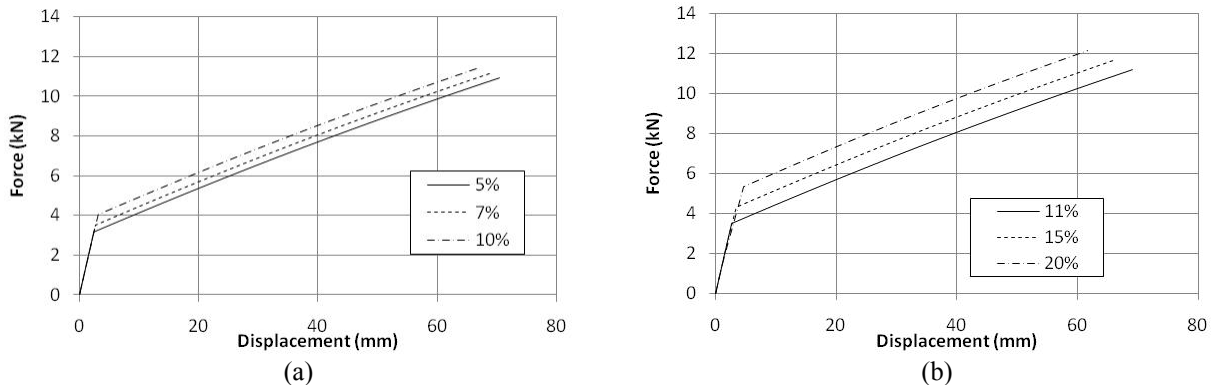


Figure 6: Lateral displacement vs. Lateral force for different (a) axial load values, and (b) post-tensioning force values

Fig. 7 illustrates the effects of changing the initial post-tensioning stresses in the rebar while keeping the total post-tensioning force constant. This was accomplished by changing the area of the post-tension rebar. It was found that a change in the initial post-tensioning stress significantly affected the post-elastic stiffness of the column. Moreover, as the cross sectional area of the post-tensioning rebar increases, ultimate strength and post-elastic stiffness increases. Conversely, as the cross sectional area of the rebar decreases, the ultimate strength and post-elastic stiffness are reduced. It should be noted, however, that varying the initial post-tensioning stress in the rebar does not affect the ultimate lateral displacement.



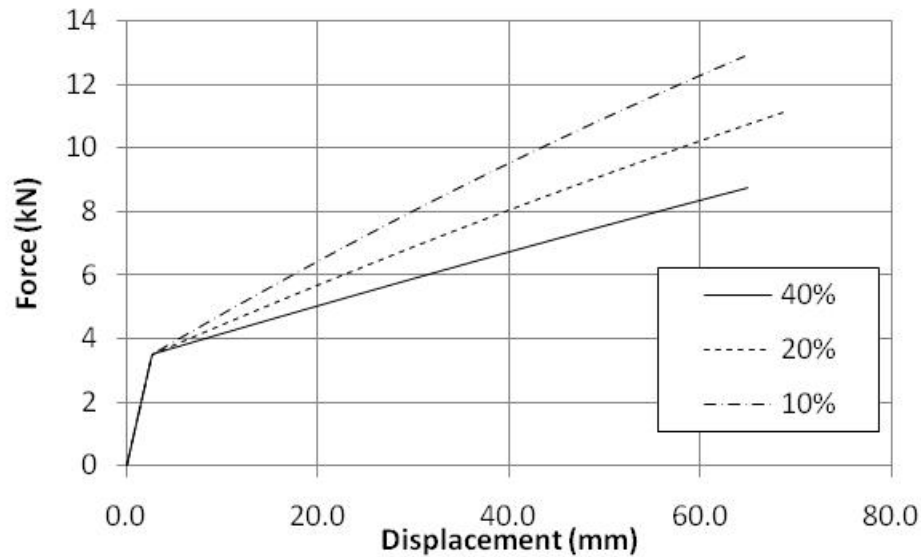


Figure 7: Lateral displacement vs. Lateral force for different initial post-tensioning stress values in the rebars

### Summary and Conclusions

This paper presents a finite element model for a cantilever column composed of segmental precast post-tensioned concrete filled fiber tubes (PPT-CFFT). Three dimensional nonlinear finite element analyses using Abaqus\Standard have been performed and a stress-strain relationship for confined concrete was used to model the concrete. The model was calibrated against cyclic tests on single-column pier and was found to accurately capture the general performance of the column. However, careful consideration must be taken when selecting the type of the contact surface between the core concrete and FRP as well as between the core concrete and the foundation. The finite element results indicated that increasing the applied post-tensioning force increases the ultimate strength and decreases the ultimate displacement. It was also shown that for a constant post-tensioning force, increasing the rebar cross sectional area increases the post-elastic stiffness and ultimate strength. with no significant change in the displacement capacity.

### Acknowledgements

Funding for this research was provided by Transportation Northwest (TransNow) under Project No. 5200. Their assistance is greatly appreciated.

### References

- Chou, C. and Chen, Y. 2006. Cyclic tests of post-tensioned precast CFT segmental bridge columns with unbonded strands, *Earthquake engineering and structural dynamics*, 35, 159-175.
- Dawood H., (2010). Modeling of self-centering CFFT columns under seismic loads, M.Sc. thesis, Washington State University
- ElGawady M., Booker, A., Dawood H. (2010a). Seismic behavior of post-tensioned concrete filled fiber tubes, ASCE, *Composites for Construction J.*
- ElGawady, M. A., Sha'lan, A., Dawood, H. (2010b). Seismic behavior of segmented bents, *proceeding of the 9<sup>th</sup> US National and 10<sup>th</sup> Canadian Conference on Earthquake Engineering Conference*,

Toronto, Canada

- ElGawdy M., Booker, A. (2009). Static cyclic response of concrete filled fiber tubes, *proceeding of FRPRCS-9*, Sydney, Australia
- ElGawady M., Ma Q., Ingham J., Butterworth J. 2006. The effect of interface material on the dynamic behavior of free rocking blocks, *8<sup>th</sup> NCEE*, EERI, San Francisco, CA.
- ElGawady M., Ma Q., Ingham J., Butterworth J. 2005. Experimental investigation of rigid body rocking, *The New Zealand Concrete Ind. Conf.*, Auckland, 2005, p.1-8
- Fam, A. Pando, M, Filz, G. and Rizkalla, S. 2003. Precast piles for Route 40 Bridge in Virginia using concrete-filled FRP tubes, *PCI journal*, 48(3), 32-45.
- Hewes, J. T.; and Priestley N., 2002. Seismic design and performance of precast concrete segmental bridge columns, *Report No. SSRP-2001/25*, Univ. of California at San Diego.
- Kwan, W.; and Billington, S. 2003. Unbonded posttensioned concrete bridge piers I: monotonic and cyclic analyses, *Journal of Bridge Engineering*, 8 (2), 92- 101
- Lee, K.; and Billington, S. In print. Residual Displacement Prediction for Structural Concrete Columns under Earthquake Loading, *ASCE, J. Bridge Engineering*
- Marriott, D., Pampanin, S., Palermo, A., 2009. Quasi-static and pseudo-dynamic testing of unbonded post-tensioned rocking bridge piers with external replaceable dissipaters, *Earthquake Engineering & Structural Dynamics*, 38(3).
- Ou, Y.; Chiewanichakorn, M.; Ahn, I.; Aref, A.; Chen, S.; Filiatrault, A.; and Lee, G. 2006. Cyclic performance of precast concrete segmental bridge columns, *TRR J.*, 1976, 66-74 pp.
- Priestley N., Sritharan S., Conley J., and Pampanin S., 1999, *Preliminary results and conclusions from the PRESSS five-story precast concrete test building*, *PCI Journal*, 44 (6):p. 42-76.
- Rouse, J., 2009. Self-Centering Bridge Piers with Structural Fuses, *Mid-Continent Transportation Research Symposium*, Ames, Iowa.
- Seible, F., Priestley, M. J. N., Chai, Y. H. 1995. Earthquake Retrofit of Bridge Columns with Continuous Carbon Fiber Jackets, Advanced Composites Technology Transfer Consortium, *Report No. ACTT-95/08*, La Jolla, California.
- Zhu, Z., Ahmad, I., and Mirmiran, A., 2006. Seismic Performance of Concrete-Filled FRP Tube Columns for Bridge Substructure, *Journal of Bridge Engineering* 11 (3), 359-370.